

Capillarity and Wetting of Carbon Nanotubes

E. Dujardin, T. W. Ebbesen,* H. Hiura, K. Tanigaki

The wetting and capillarity of carbon nanotubes were studied in detail here. Nanotubes are not "super-straws," although they can be wet and filled by substances having low surface tension, such as sulfur, selenium, and cesium, with an upper limit to this tension less than 200 millinewtons per meter. This limit implies that typical pure metals will not be drawn into the inner cavity of nanotubes through capillarity, whereas water and organic solvents will. These results have important implications for the further use of carbon nanotubes in experiments on a nanometer scale.

A feature of carbon nanotubes that offers intriguing possibilities for future research is the inner hollow cavity. Only a few nanometers in diameter and a few micrometers in length, such a cavity should allow for interesting nanoscale experiments if it could be filled with other materials in a systematic way through capillarity. For instance, the cavity could act as a nanometer-size test tube with motions restricted to a low dimensional environment. It could also be used as a nanometer-size mold to make quantum wires. [Zeolites have been extensively studied for such purposes (1-3).] However, little is known about the capillarity and wetting of nanotubes, which is essential for practical use of this inner cavity.

Theoretical calculations first predicted that open nanotubes should act as "nanostraws" and draw in molecules from vapor or fluid phases (4). It was then demonstrated that when reacting with lead and air closed nanotubes could be filled by a lead compound (5). However, in subsequent experiments we found that if nanotubes were first opened at their tips and exposed to molten lead or other metals in an inert atmosphere, these were not drawn in by capillarity (6). We suggested at the time that debris at the entrance of the open nanotubes or pressure differences might account for the differences in the results (6). However, there may be other reasons (7).

The key to this problem is the surface energies of the interaction between the liquid and the solid surface of the nanotube. This is a problem of wetting, for wetting and capillarity are intimately related (8). Wetting is necessary for observing capillary action, as can be understood from the Laplace equation

$$\Delta P = \frac{2\gamma\cos\Theta}{r} \quad (1)$$

where r is the radius of curvature, ΔP the

pressure difference across the liquid-vapor interface, γ the surface tension, and Θ the liquid-solid contact angle. The size of the contact angle Θ , shown in Fig. 1, is critical because ΔP will be negative if Θ is larger than 90° . In such a case, the contact angle is said to be nonwetting and pressure must be applied to cause the liquid to enter the tube. So, if one wanted to fill nanotubes with a given substance by capillarity, the substance must have a contact angle $<90^\circ$. However, it is not easy to predict the contact angle, which is related to the interfacial tensions such that

$$\cos\Theta = \frac{\gamma_{SV} - \gamma_{SL}}{\gamma} \quad (2)$$

where γ_{SV} and γ_{SL} indicate the tensions at the solid-vapor and solid-liquid interfaces, respectively. Furthermore, it is not clear whether these, and other related equations, hold for capillaries as small as the nanotubes (3, 9, 10). In general, it can be said that the polarizability of the solid should be higher than that of the liquid for good

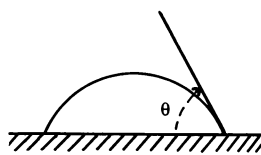


Fig. 1. Contact angle Θ of a liquid on a solid surface.

Table 1. Surface tensions of various elements and their wetting ability of nanotubes. The values for γ , taken from (21), should be seen as approximate (within 5%) because there is a spread in the reported values.

Element	γ (mN/m)	Wetting
S	61	Yes
Cs	67	Yes
Rb	77	Yes
Se	97	Yes
Te	190	No
Pb	470	No
Hg	490	No
Ga	710	No

wetting (9). In practice, it is possible to screen potential candidates for capillarity by first seeing if they will wet the outside of nanotubes in the bulk, as described below.

The nanotubes were synthesized by the carbon arc method (11, 12). The nanotube sample, taken from the core of the carbon arc deposit, was then ground with a mortar and pestle and placed in the bottom of a glass tube. The substance to be tested was placed on top of the nanotubes, generally in a powder form. The glass tube was then evacuated and sealed. (For very reactive substances, such as alkali metals, the procedure was carried out in a glove box.) The sealed tube containing the nanotubes and the element was then placed in an oven in order to melt the element and see whether it would wet the nanotube bulk material.

Our results were clear: when the substance did not wet, it generally formed a ball on top of the nanotubes (like mercury on a glass surface). When it did wet, it was absorbed into the bulk nanotube material trying to fill the cavities between the nanotubes or nanoparticles. The driving force for this process was the pressure difference across the curved meniscus of the liquid in the cavities (akin to a capillary rise) (8). The samples were then checked with a high-resolution transmission electron microscope (TEM) (Fig. 2) to identify the wetting of the outside surfaces of nanotubes. As an example of the results, Fig. 2 shows the wetting of the nanotube by sulfur. It was difficult to determine a contact angle because the sulfur solidified on the surface into various shapes and angles.

Table 1 summarizes our wetting experiments together with the surface tension of the elements used. From these results, it is clear that high surface tension materials such as metals and transition metals do not wet nanotubes. Therefore, these will also

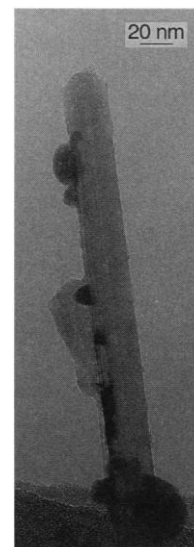


Fig. 2. Carbon nanotubes wet by sulfur. The sulfur appears as darker aggregates on the outer surfaces of the nanotubes.

Fundamental Research Laboratories, NEC Corporation, 34 Miyukigaoka, Tsukuba 305, Japan.

*To whom correspondence should be addressed at NEC Research Institute, 4 Independence Way, Princeton, NJ 08540, USA.

not be drawn in by capillary forces into the inside cavity of the nanotubes. On the other hand, it was apparent that low surface tension materials wet the surface despite their chemical nature because we find in this category elements from opposite ends of the periodic table. Therefore, the determining factor for wetting appears to be surface tension, with the cutoff point between 100 and 200 mN/m. This cutoff is probably not sharp because typical samples contain a distribution of tubes having different diameters and helicities, which are expected according to calculations (13–16) to have different electronic properties. Only when the nanotube diameter is very large will its properties, such as wetting, approach those of graphite.

The next question we investigated was whether the wetting elements with low surface tension are also drawn in by capillarity into the inside of the nanotubes. To check this, we opened the nanotubes by oxidizing their tips in air at 750°C (6). The opened nanotubes were then placed in one compartment of a two-compartment glass tube. In the other compartment, the element was introduced, and the whole system was evacuated to 10^{-7} torr. Then, only the compartment containing the nanotubes was heated to 1000°C for a couple of hours while it was continuously evacuated in order to remove residual gases that might be left from the oxidation process. The system was cooled, and the element from the other compart-

ment was transferred in situ to the nanotube compartment. The sealed mixture was then heated beyond the melting point of the element for a few hours.

The TEM pictures in Fig. 3 show our results, with the open nanotubes filled through capillarity. This can be most easily seen for Se (Fig. 3A) and to a lesser degree for Cs (Fig. 3, B and C), both of which give strong image contrasts. As can be seen in Fig. 3A, the Se has entered from the open tip and filled entirely the first compartment of the nanotube. At the tip, the excess Se has solidified with a crystalline structure including defect lines. Selenium is also found along the outside surface of the nanotube as expected because wetting is a prerequisite for capillary action. The Cs-filled samples had to be exposed to air and sonicated in ethanol solution before TEM imaging, so that most of the Cs must have reacted to form oxide and dissolved away. Probably for that reason, the Cs (or its oxide) has a particulate structure (Fig. 3, B and C). In Fig. 3B, the materials appear to be on the outside, whereas in Fig. 3C, particles are seen only inside the hollow cavity, far from the entrance at the tip.

From these results, we can draw a number of conclusions. Only relatively low surface tension materials will be drawn inside carbon nanotubes by capillary forces. The ability to wet reflects the competition between the cohesive forces in the liquid and the strength of the interactions of the liquid

with the surface. Therefore, it is perhaps only natural that liquids with low surface tension should wet more easily. If possible, theoretical calculations should take into account the energy gain from wetting to give a more accurate prediction of the capillarity of nanotubes.

Earlier results, where closed nanotubes were filled in the presence of lead (5) or bismuth (6) in an oxidizing environment, are best explained by the fact that the metal reacted with the oxygen or carbon to form a compound with sufficiently low surface tension to be drawn in by capillarity. If pure metals, such as Pb, are to be introduced into the nanotubes, outside pressure must be applied. The pressure required will depend on the diameter of the tube and the contact angle, as can be seen from Eq. 1. For instance, to fill a 1-nm-diameter nanotube with liquid Pb, pressures of the order of 1000 to 10,000 atm will be required, depending on the contact angle. If the sample is then cooled with the pressure on, the Pb will be stuck inside the nanotubes. This might be one approach for filling nanotubes with a desired metal in a systematic way to form nanocomposites. Metal or metal carbides are occasionally found inside nanotubes produced with an arc with metal-filled carbon electrodes (17–20). Although the surface tensions will be lower at higher temperatures of the arc, the filling is most likely not a result of capillary action. As has been pointed out, the contact angles indicate a nonwetting behavior (18, 19).

The wetting cutoff value for surface tension is still sufficiently high to allow wetting by water ($\gamma \sim 72$ mN/m) and most organic solvents ($\gamma < 72$ mN/m). For instance, the bulk material of nanotubes is readily wet by water. So in principle, it is possible to do solution chemistry (chemical catalysis and low dimensional chemistry, for example) inside opened nanotubes. Nanotubes could also find use in biomimetic systems because tubular structures, such as tubulin, serve important functions in living organisms.

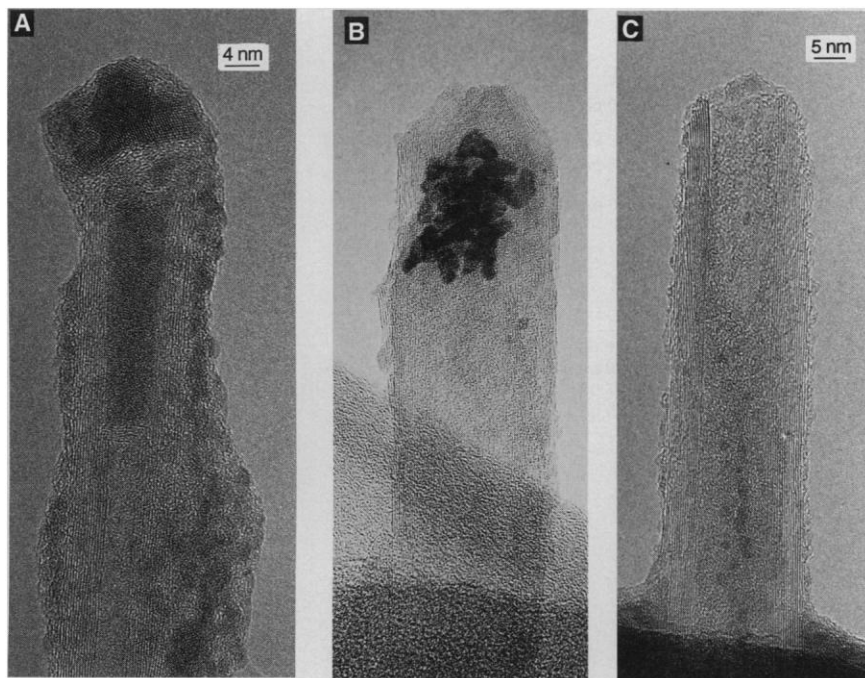


Fig. 3. Transmission electron microscope images of filled nanotubes. (A) Selenium has filled the first hollow compartment of the nanotube, entering from the tip. Selenium can also be seen on the outside surface of the nanotube, where it appears globular, and at the tip, where the excess has crystallized. (B and C) Cesium, or cesium oxide, can be seen as small dark particles on the outside surface of a nanotube (B) and in the inside hollow (C).

REFERENCES

1. G. D. Stucky and J. E. Mac Dougall, *Science* **247**, 669 (1990).
2. T. Sun, K. Seff, N. H. Heo, V. P. Petranovskii, *ibid.* **259**, 495 (1993).
3. V. N. Bogomolov, *Sov. Phys. Tech. Phys.* **37**, 79 (1992).
4. M. R. Pederson and J. Q. Broughton, *Phys. Rev. Lett.* **69**, 2689 (1992).
5. P. M. Ajayan and S. Iijima, *Nature* **361**, 333 (1993).
6. P. M. Ajayan *et al.*, *ibid.* **362**, 522 (1993).
7. T. W. Ebbesen, *Annu. Rev. Mater. Sci.* **24**, 235 (1994).
8. A. W. Adamson, *Physical Chemistry of Surfaces* (Wiley-Interscience, New York, 1990).
9. P. G. de Gennes, *Rev. Mod. Physics* **57**, 827 (1985).
10. D. Quéré, J.-M. di Meglio, F. Brochard-Wyart, *Science* **249**, 1256 (1990).
11. T. W. Ebbesen and P. M. Ajayan, *Nature* **358**, 220 (1992).

12. T. W. Ebbesen *et al.*, *Chem. Phys. Lett.* **209**, 83 (1993).
13. N. Hamada, S. Sawada, A. Oshiyama, *Phys. Rev. Lett.* **68**, 1579 (1992).
14. R. Saito, M. Fujita, G. Dresselhaus, M. S. Dresselhaus, *Appl. Phys. Lett.* **60**, 2204 (1992).
15. J. W. Mintmire, B. I. Dunlap, C. T. White, *Phys. Rev. Lett.* **68**, 631 (1992).
16. X. Blase, L. X. Benedict, E. L. Shirley, S. G. Louie, *ibid.* **72**, 1878 (1994).

17. S. Seraphin, D. Zhou, J. Jiao, J. C. Withers, R. Loutfy, *Nature* **362**, 503 (1993).
18. S. Subramoney *et al.*, *Carbon* **32**, 509 (1994).
19. Y. Saito *et al.*, *J. Phys. Chem. Solids* **54**, 1849 (1993).
20. P. M. Ajayan *et al.*, *Phys. Rev. Lett.* **72**, 1722 (1994).
21. *Handbook of Physics and Chemistry* (CRC Press, Boca Raton, FL, ed. 69, 1988).

13 June 1994; accepted 29 July 1994

Two Identical Noninteracting Sites in an Ion Channel Revealed by Proton Transfer

Michael J. Root and Roderick MacKinnon

The functional consequences of single proton transfers occurring in the pore of a cyclic nucleotide-gated channel were observed with patch recording techniques. These results led to three conclusions about the chemical nature of ion binding sites in the conduction pathway: The channel contains two identical titratable sites, even though there are more than two (probably four) identical subunits; the sites are formed by glutamate residues that have a pK_a (where K_a is the acid constant) of 7.6; and protonation of one site does not perturb the pK_a of the other. These properties point to an unusual arrangement of carboxyl side-chain residues in the pore of a cation channel.

One of the major goals of mechanistic ion channel studies is to understand the nature of ion coordination sites in the pore that allow selective ion permeation. Recent progress has been made in the identification of amino acids that are responsible for ion binding in cyclic nucleotide-gated (CNG) channels and in voltage-dependent Ca^{2+} channels. CNG channels and voltage-dependent Ca^{2+} channels are only distantly related in their primary sequences, but their ion conduction properties are very similar. Most notably, both channel types contain high-affinity, divalent cation-binding sites that are important for channel function under physiological conditions (1, 2). In the case of Ca^{2+} channels, divalent cation-binding sites allow the channel to exclude monovalent cations and conduct only Ca^{2+} . In CNG channels, which are responsible for the initial electrical signals underlying visual and sensory transduction, binding of Mg^{2+} or Ca^{2+} in the pore reduces the effective, single-channel conductance. In photoreceptor cells, a small single-channel conductance ensures a smoothly graded electrical response to varying light intensity (2). In addition, the ability of Ca^{2+} to pass through CNG channels may also play a role in visual and olfactory sensory transduction (2, 3).

A similar amino acid composition in the pore-forming region (P-region) underlies the shared open-channel properties of CNG channels and Ca^{2+} channels (4). In both, divalent cation binding is mediated by a set of P-region Glu residues. Four Glu

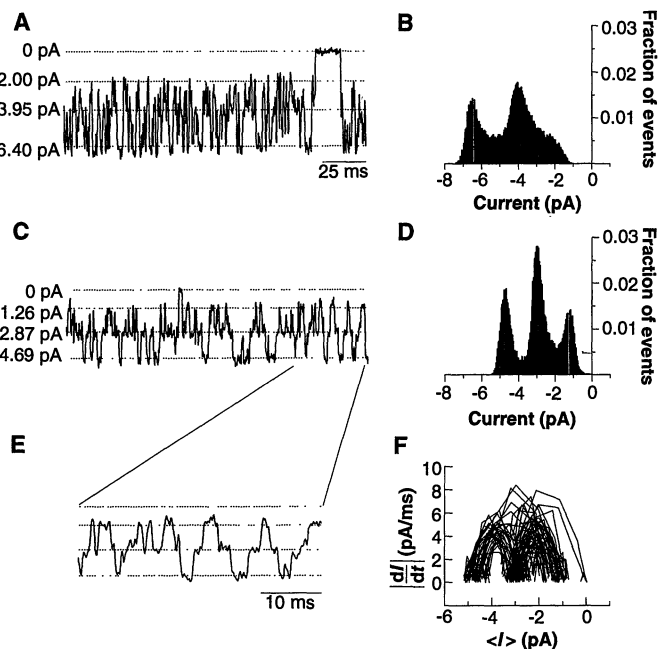
residues, one from each of the homologous domains of Ca^{2+} channels, apparently form a cluster of carboxyl groups that is capable of binding at least one (perhaps two) divalent cations (5). In an analogous fashion, a Glu residue is provided by each of the identical subunits of a CNG channel to form a divalent cation-binding site in that channel (6). To further probe the chemical groups within the pore of the CNG chan-

nel, we studied the effect of protons on ionic conduction. Our findings lead us to conclude that the P-region Glu residues are arranged so as to give rise to two identical proton-binding sites within the pore.

Experiments were done on the cloned CNG channel from catfish olfactory epithelium, expressed in *Xenopus* oocytes (7). A single channel recorded in 130 mM NaCl solution (pH 7.6, at -80 mV) is shown in Fig. 1A. The open channel showed multiple poorly resolved levels of conductance; at least three are apparent in the amplitude histogram (Fig. 1B). A similar measurement made in solutions prepared with 2H_2O (deuterium oxide) is shown in Fig. 1C. Transitions between conductance levels occur at a slower rate as a result of a kinetic isotope effect (8). Under this condition, the amplitude histogram showed three distinct peaks defining the high, middle, and low conductance states (Fig. 1D). All further experiments were carried out in solutions prepared with 2H_2O to allow a detailed study of these three states.

A closer look at the current record reveals a precise connectivity among the three states. The expanded trace in Fig. 1E shows that most transitions connecting the high and low states pause for a measurable time at the middle state. The sequential connectivity is also reflected in the transient-mean analysis (Fig. 1F). Transitions appear as trajectories connecting the current levels (9). The double-arched appearance of the plot reflects a high density of trajectories connecting the middle state

Fig. 1. Fluctuations of current through single olfactory CNG channels (21). (A and C) Currents were measured at a membrane potential of -80 mV with 130 mM NaCl on both sides of the membrane (22). Solutions were prepared with H_2O (A) and 2H_2O (C) titrated to a pH of 7.6. The closed-state current is designated by the 0 pA line. (B and D) Open-state amplitude histograms of the channels in (A) and (C), respectively. The bin width is 0.049 pA (twice the resolution of the analog-digital converter), and the bins were normalized by the total number of measured points [39196 for (B) and 33792 for (D)]. (E) Part of the trace in (C) has been expanded to reveal the transitions between extreme conductance states. (F) For a three-point window moving along the trace in (C), the absolute value of the time derivative is plotted as a function of the mean current. Transitions between current levels in the time trace become parabolic trajectories in this transient-mean analysis (9).



Department of Neurobiology and the Biophysics Program, Harvard Medical School, Boston, MA 02115, USA.